Electronic Supplementary Material (ESI) for Nanoscale.
This journal is © The Royal Society of Chemistry 2024

The Supplementary Materials for: "Strain-mediated multistate skyrmion for neuron devices"

Shengbin Shi[a], Yunhong Zhao[b], Jiajun Sun[a], Guoliang Yu[c], Haomiao Zhou[c] and Jie Wang*[,a,b,d]

[a]Department of Engineering Mechanics, Zhejiang University, Zheda Road 38, Hangzhou, Zhejiang 310027, China;

[b]Zhejiang Laboratory, Hangzhou 311100, Zhejiang, China;

[c]Key Laboratory of Electromagnetic Wave Information Technology and Metrology of Zhejiang Province, College of Information Engineering, China Jiliang University, Hangzhou 310018, People's Republic of China

[d]Key Laboratory of Soft Machines and Smart Devices of Zhejiang Province, Zhejiang University, Zheda Road 38, Hangzhou, Zhejiang 310027, China;

*Corresponding Authors:

Dr. Jie Wang

Email: jw@zju.edu.cn

Figure S1

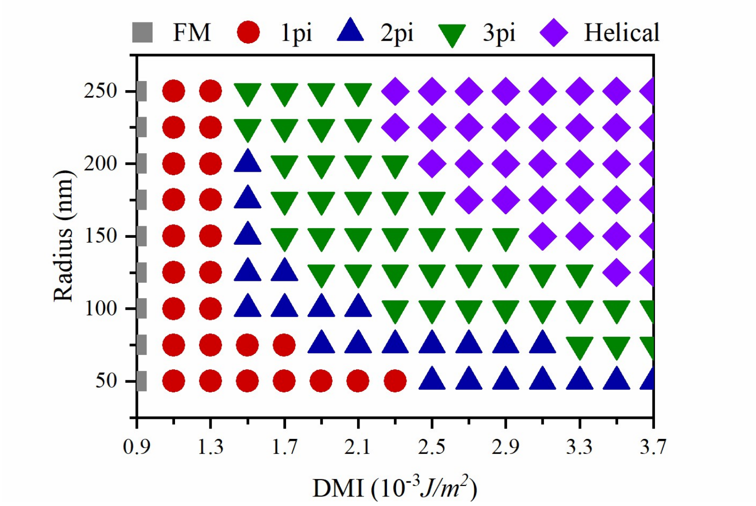

Fig. S1. Relaxed states in Co nanodisc with different radius and DMI coefficients

In order to select a suitable material system for the kπ skyrmion switching process, the disc size and DMI coefficients were systematically explored with a fixed K_1 of 0.32. As shown in Figure S1, the radius and DMI coefficients deeply affect the relaxed states of the Co nanodisc. The overlarge or excessively low DMI coefficients cannot induce kπ skyrmion on the basis of energy minimization principle. This provides a reference for the selection of suitable device size and DMI coefficient in this work.

Figure S2

As shown in Figure S2, when the highest state is 2π skyrmion, only one-step transformation is required to fully return to a single domain, corresponding to the same magnetization direction of initial state. That is, if the value of k corresponding to the highest state is an even number, for example, k=2, the magnetization of final state can be returned to the initial state after the reset.

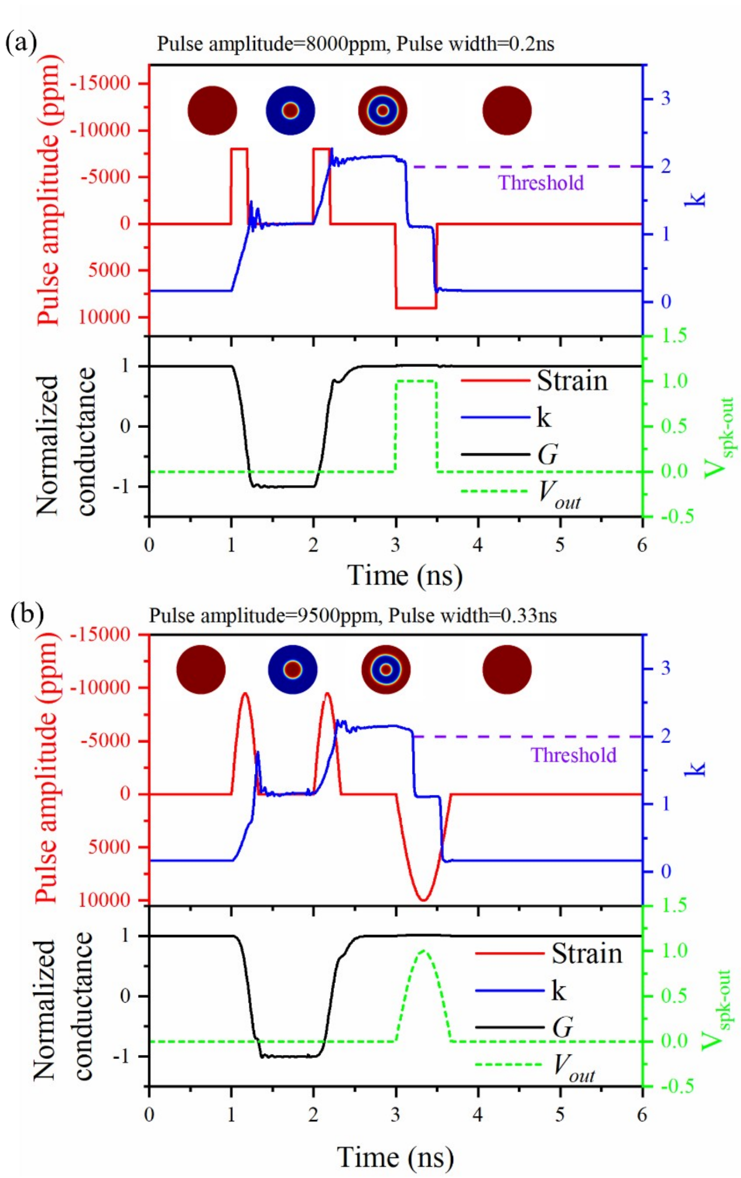

Fig. S2. Demonstration of IF behavior of the proposed skyrmionic neuronal device applied with (a) regular square strain pulse and (b) bioplausible strain pulse, respectively, when the threshold is preset as k=2.

Figure S3

Because the skyrmion nucleation requires a certain amount of energy, the strain pulse with appropriate width and amplitude can induce the state transformation of $k\pi$ skyrmion. Figure S3 shows the critical strain amplitude applied to the Co nanodisc varies with the DMI coefficient, in order to generate the change from the appointed initial state to the desired state of $k\pi$ skyrmion with a disc diameter of 400 nm and the sufficient pulse width. When the DMI coefficient is larger, the strain amplitude required for the state transformation from k to k+1 is smaller. Also, for the same DMI coefficient, the strain amplitude is higher required to change the state to the higher one. In contrast, the larger the DMI coefficient, the larger the strain amplitude is required for annihilation of the kπ skyrmion. Besides, the strain amplitude is higher required to change the state to the lower one with the same DMI coefficient. It is worth noting that when the DMI coefficient is between 1.1 and 1.5, the spin-orbit coupling is too small to stabilize the 3π skyrmion. that is, it can be annihilated into 2π or 1π without an external field. Under the condition denoted with the yellow region, the process from k=3 to k=2 cannot be obtained due to the instability of 2π skyrmion.

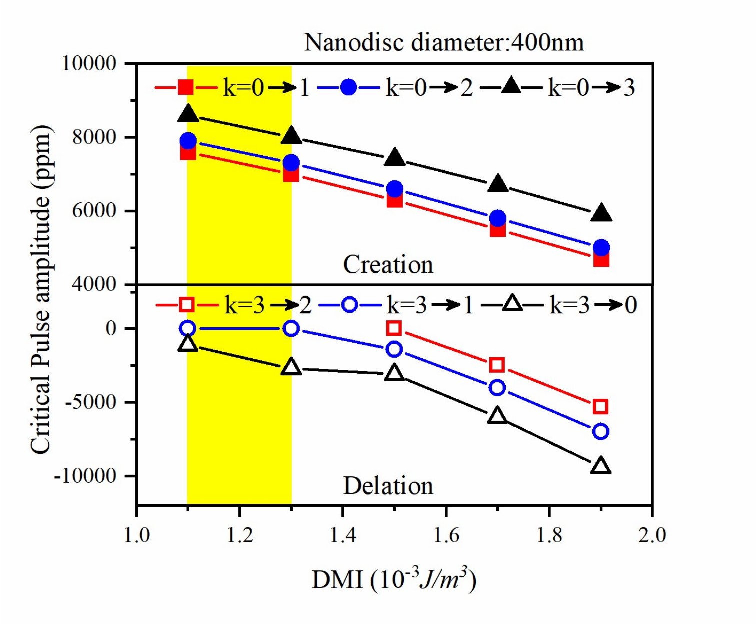

Fig. S3. The critical strain amplitude applied to the Co nanodisc to generate the change from the appointed initial state to the desired state of kπ skyrmion as a function of DMI coefficients.

Figure S4

In order to verify the robustness of the temperature perturbation, we added a randomly perturbed temperature field in the phase field model[1]. The temperature field is expressed as:

$$H_{therm} = \vec{\eta}(step)\sqrt{2\mu_0 \alpha k_B T / (M_{sat} \gamma_{LL} \Delta V \Delta t)}$$

Where α is the damping parameter, k_B is the Boltzmann constant, T is the temperature, M_{sat} is the saturation magnetization, $\vec{\eta}(step)$ is a random vector form based on a standard normal distribution and the value is changed after every time step.

Referring to the material parameters and operation methods in Fig. 4(a) in the manuscript, the effect of temperature is considered in Figure S4. When the temperature varies from 0 to 10 K, the IF function is still maintained well as shown in Figure S4, which may be attributed to the almost constant saturation magnetization in the low temperature[2]. Although the temperature perturbation interferes with the accuracy of the k calculation through the vertical magnetization angle, it does not affect the detection of the magnetization direction by the MTG. It shows that the IF function of this neural unit **is not affected in the** low **temperature range**.

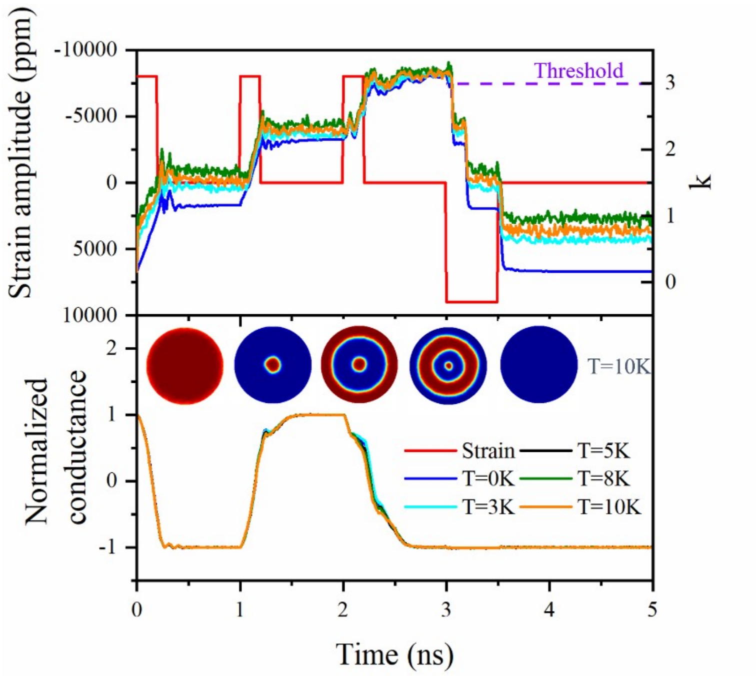

Fig. S4. The realization of IF function of skyrmionics based neural device with the temperature varying from 0 to 10 K.

Notes S1: the parameters of the magnetic material

To investigate the states of strain-manipulated skyrmion, a mesh cell size of $2\,nm \times 2\,nm \times 1\,nm$ is used to discretize the simulated model. The magnetic material parameters used for the simulations are obtained from the relevant literatures[3-

[5]. $M_s = 0.58 \times 10^6\ Am^{-1}$, $A_{ex} = 15 \times 10^{-12}\ Jm^{-1}$, $D = 1.6 \times 10^{-3}\ Jm^{-2}$, $K_1 = 0.32 \times 10^6\ Jm^{-3}$, $K_2 = 0$, $\alpha = 0.01$, $B_1 = -6.51 \times 10^6\ Nm^{-2}$, $B_2 = 0\ Nm^{-2}$, $\upsilon = 1/3$. The values of K_1 and D deeply affect the magnetic states as shown in the Supplementary Figure 1, the reasonable selection of which is vital to design multistate switching in the ferromagnetic materials [6]. For simplicity, the parameters of the magnetic material chosen here at the ideal low temperature T = 0 K, neglecting the the effect of temperature.

Notes S2: Mechanism for varying the amplitude and width of the strain pulse to modulate the $k\pi$ skyrmion

In the simulation of micromagnetic simulation, the strain is equivalent to the effective magnetic field after magnetoelastic coupling, which can be equal to the following equation in perpendicular anisotropy [7].

$$K_\varepsilon = B_1\left(1 + \frac{2c_{12}}{c_{11}}\right)\varepsilon_{amp} \qquad (S1)$$

Where $\varepsilon_{amp}(=\varepsilon_{xx}=\varepsilon_{yy})$ [8] is the applied biaxial in-plane strain. Therefore, the larger the pulse amplitude is, the easier it is to turn the single domain into skyrmion states. As we all known, the magnetization evolution takes time and the application time of strain depends on the pulse width. When the magnetic domain evolves to the specified state and is about to the next state, it will keep the current state due to the energy barriers between the different states if the strain is withdrawn. So we can change the pulse width and the amplitude to regulate the skymions states, in order to realize the increase or decrease of k number.

Notes S3: the MNIST pattern recognition parameters

The neurons of the SNN are organized into a structure of 784 × 128 × 10, where an input layer, a hidden layer and an output layer are connected as shown in Fig. 5(a). The skyrmionic SNN is trained on the 50000 images and tested on the 10000 images, which comes from the MNIST handwritten data set consisting of ten classes (numbers $0 \rightarrow 9$) on a grid of 28×28 pixels. Each image is reshaped into a column vector corresponding to the input dimension of the SNN. In our simulations, a Poisson coding scheme is used, where each item in the column vector is set to the probability generating a pulse with time step of 1 ns based on the pixel value. After 50 ns, we obtain a pulse sequence, transforming an image into a 784×50 matrix. At each time step, the neuronal device receives a voltage pulse from the pre-neuron, which causes the state of the skyrmion to change according to the following equation:

$$K_i(t) = K_i(t-1) + \kappa\left(\sum_j w_{ij} x_j(t) + b_j\right) \qquad (S2)$$

where $K_i(t)$ is the state of the skyrmion in the i-th neuron and $x_j(t)$ is the presynaptic spike from the j-th neuron. The presynaptic spikes are weighted by the synaptic device (w_{ij}). The skyrmion in the neuronal device varies per unit voltage pulse κ. Since the device shows significant linearity and the step-by-step process, it is reasonable to implement the integral $\kappa(t) = \Delta t \left\lfloor \sum_j w_{ij}\, x_j(t)) \right\rfloor$ by using a first-order Taylor expansion and rounding down, where Δt is the 1 ns time step. The superimposed form of multiple strain pulses at a time step and the transformation of skyrmion states are explained in detail in Supplementary Table S1.

Table S1:

Table S1. Superposition rules of multiple pulses (Standard pulse: 8000 ppm/0.2 ns or 8600 ppm/0.2 ns)

Initial state	Pulse numble	Superimposed pulse width (ns)	Superimposed pulse form (pulse with /ns)	Final state	Changes of state
0π	1	0.2	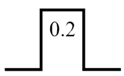	1π	1
0π	2	0.35	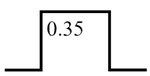	2π	2
0π	3	0.49	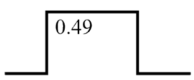	3π	3

1π	1	0.2	0.2	2π	1
1π	2	0.2+0.2	0.35	3π	2
2π	1	0.2	0.2	3π	1

When the multiple strain pulses swarm in the same time step of the pulsed neural network, the state change of the skyrmion is described in the Table S1. Here, for the convenient regulation, the pulse width is merely considered in the superposition rules of multiple pulses. The standard pulse is preset with the width of 0.2 ns and the amplitude of 8000 or 8600 ppm. If two pulses arrive in the same time step, the superimposed width of strain pulse is 0.35 ns. Similarly, if three pulses arrive, the superimposed width of strain pulse is 0.49 ns. Here, in particular, if the initial state is non-ferromagnetic, the strain amplitude needs to be adjusted from 8000 ppm to 8600 ppm, due to an additional bias stress required for the ferromagnet in a metastable state[9].

Supplementary Movie 1: Demonstration of IF behavior of the proposed skyrmionic neuronal device applied with regular square strain pulse when the threshold is preset as k = 3.

Supplementary Movie 2: Demonstration of IF behavior of the proposed skyrmionic neuronal device applied with regular square strain pulse when the threshold is preset as k = 2.

Supplementary references:

1. A. Vansteenkiste, J. Leliaert, M. Dvornik, M. Helsen, F. Garcia-Sanchez and B. Van Waeyenberge, *AIP Adv.*, 2014, **4**, 107133.
2. V. M. Parakkat, K. Ganesh and P. Anil Kumar, *AIP Adv.*, 2016, **6**.
3. J. Sun, S. Shi and J. Wang, *Advanced Engineering Materials*, 2021, DOI: 10.1002/adem.202101245.
4. J. Sampaio, V. Cros, S. Rohart, A. Thiaville and A. Fert, *Nat. Nanotechnol.*, 2013, **8**, 839-844.
5. G. Yu, X. Xu, Y. Qiu, H. Yang, M. Zhu and H. Zhou, *Appl. Phys. Lett.*, 2021, **118**, 142403.
6. X. Liu, Q. Zhu, S. Zhang, Q. Liu and J. Wang, *AIP Adv.*, 2015, **5**.
7. J.-M. Hu, T. Yang and L.-Q. Chen, *npj Computational Materials*, 2018, **4**.
8. J.-M. Hu, C.-W. Nan and L.-Q. Chen, *Phys. Rev. B*, 2011, **83**.
9. S. Li, Q. Li, J. Liu, N. Ran, P. Lai, L. Shen, J. Xia, L. Xie, Y. Zhou and G. Zhao, *Phys. Rev. B*, 2023, **107**.